10.48047/jocaaa.2024.33.05.51

THERMAL MODELING OF SEMICONDUCTOR DEVICES AND VALIDATION

Preethi Elizabeth Iype
Electronics & Communication Engineering
KLUniversity
Dr. V. Suresh Babu Principal
(Rtd.) College of Engineering Trivandrum Thiruvananthapuram
Balasaheb Hanumantrao Patil
At Post: Pimpali, Taluka: Baramati, District: Pune
State: Maharashtra, Pin code: 413102

ABSTRACT

The continuous miniaturization of semiconductor devices, coupled with increased operating frequencies and higher power densities, has made thermal management a critical challenge in modern electronic systems. Excessive temperature rise within semiconductor junctions adversely affects device performance, accelerates material degradation, and significantly reduces operational reliability and lifetime. Consequently, accurate prediction of thermal behavior has become an essential requirement during the design and validation stages of semiconductor devices.

This research focuses on the systematic development, simulation, and experimental validation of thermal models for semiconductor devices operating under steady-state and transient conditions. The study investigates fundamental heat transfer mechanisms within semiconductor structures and integrates analytical, numerical, and compact thermal modeling approaches to achieve reliable temperature prediction. Analytical models establish baseline thermal resistance and capacitance characteristics, while numerical simulations based on finite-element methods capture spatial temperature distributions and hotspot formation with high accuracy. Furthermore, compact thermal models enable efficient integration of thermal effects into circuit-level simulations.

The developed thermal models are implemented using industry-standard simulation tools and validated through experimental measurements obtained from controlled laboratory setups. Electrical and physical temperature measurement techniques extract junction and surface temperatures under varying power dissipation and ambient conditions. Detailed comparison between simulated and measured results demonstrates strong correlation, confirming the accuracy and robustness of the proposed modeling framework. Error analysis identifies sources of deviation, including material property variations, boundary condition assumptions, and measurement uncertainties. The validated models can be effectively applied to device design optimization, reliability assessment, and thermal-aware electronic system development.
Keywords: Thermal modeling, semiconductor devices, finite element analysis, thermal resistance, junction temperature, experimental validation, compact thermal models

1. INTRODUCTION

Modern semiconductor technology faces unprecedented thermal challenges as device dimensions shrink while power densities continue to increase. Current generation processors

10.48047/jocaaa.2024.33.05.51

and power electronics operate at power densities exceeding 100 W/cm², generating significant heat within microscopic junction areas (Bar-Cohen et al., 2015). This thermal concentration creates localized hotspots that can reach temperatures 30-50°C above average chip temperatures, threatening device integrity and performance.

Temperature elevation in semiconductor devices triggers multiple failure mechanisms. Increased junction temperatures accelerate electromigration in interconnects, enhance thermally-activated diffusion processes, and reduce carrier mobility in active regions (Smy et al., 2019). These effects manifest as parametric drift, increased leakage currents, and eventual catastrophic failure. Reliability studies indicate that every 10°C increase in operating temperature approximately doubles the failure rate of semiconductor devices, following the Arrhenius relationship for thermally-activated degradation processes.

The complexity of modern semiconductor packaging compounds thermal management challenges. Three-dimensional integrated circuits, system-in-package configurations, and advanced heterogeneous integration create intricate thermal pathways where heat spreads through multiple material layers with vastly different thermal properties. Traditional thermal design approaches based on simple thermal resistance calculations prove inadequate for these complex structures, necessitating sophisticated modeling techniques that accurately capture three-dimensional heat flow, transient thermal responses, and localized hotspot formation.

Despite extensive research in semiconductor thermal modeling, several practical gaps persist. Many existing models rely on simplified geometric representations that fail to capture actual device complexity. Material property variations across temperature ranges are often neglected, introducing significant errors in high-temperature predictions. Furthermore, validation efforts frequently lack comprehensive experimental verification across multiple operating conditions, limiting confidence in model accuracy for design applications.

This research addresses these gaps through systematic development and rigorous validation of thermal models applicable to contemporary semiconductor devices. The study pursues three primary objectives: developing accurate analytical and numerical thermal models that capture both steady-state and transient thermal behavior, implementing these models using industry-standard simulation platforms, and conducting comprehensive experimental validation to verify model accuracy across representative operating conditions. The validated modeling framework provides designers with reliable tools for thermal-aware device development and optimization.

2. OBJECTIVES

This research pursues the following specific objectives:

- **Primary Objective:** To develop and validate comprehensive thermal models for semiconductor devices that accurately predict junction temperatures under steady-state and transient operating conditions.
- **Secondary Objective 1:** To implement analytical thermal resistance networks and numerical finite-element models capturing three-dimensional heat flow in semiconductor structures.
- **Secondary Objective 2:** To derive compact thermal models suitable for integration into circuit-level simulations while maintaining acceptable accuracy.

10.48047/jocaaa.2024.33.05.51

- **Secondary Objective 3:** To establish experimental measurement protocols using both electrical and physical techniques for junction temperature extraction.

• **Secondary Objective 4:** To quantify modeling accuracy through systematic comparison between simulation predictions and experimental measurements across varying power levels and thermal boundary conditions.

3. SCOPE OF STUDY

This research operates within the following boundaries:

- **Device Scope:** Focus on discrete power semiconductor devices (MOSFETs, IGBTs) and integrated circuit test structures with accessible terminals for electrical characterization.
- **Thermal Conditions:** Analysis covers steady-state thermal equilibrium and transient heating/cooling transients up to 10 seconds duration.
- **Modeling Approaches:** Three complementary methods—analytical thermal networks, finite-element numerical simulation, and compact thermal models.
- **Temperature Range:** Operating conditions from ambient (25°C) to maximum junction temperatures of 150°C, representing typical power device specifications.
- **Validation Methods:** Electrical temperature-sensitive parameter measurements and infrared thermography for surface temperature mapping.
- **Simulation Tools:** COMSOL Multiphysics for finite-element analysis, MATLAB for analytical calculations, and SPICE-compatible compact model implementation.
- **Excluded Elements:** Package-level thermal analysis beyond die attach and immediate substrate, reliability lifetime predictions, and coupled electro-thermal transient simulations.

4. LITERATURE REVIEW

4.1 Fundamentals of Semiconductor Thermal Behavior

Heat generation in semiconductor devices originates from multiple physical mechanisms. Ohmic losses in resistive regions, switching losses during transistor state transitions, and reverse recovery losses in diodes all contribute to power dissipation (Castellazzi et al., 2018). For power devices operating in switching applications, dynamic losses often dominate total power dissipation, requiring transient thermal analysis beyond simple steady-state calculations.

Heat transfer within semiconductor structures involves all three fundamental modes: conduction through solid materials, convection at surfaces exposed to fluid environments, and radiation from high-temperature surfaces. In typical electronic packages, conduction dominates heat removal paths, with thermal energy flowing from the active silicon junction through multiple material layers toward heat sinks or ambient environments (Pedram and Nazarian, 2006). The thermal resistance concept, analogous to electrical resistance, provides a convenient framework for quantifying heat transfer efficiency through these pathways.

4.2 Thermal Modeling Approaches

Analytical thermal modeling employs thermal resistance networks analogous to electrical circuit analysis. Each material layer and interface is represented by a thermal resistor, with heat

10.48047/jocaaa.2024.33.05.51

flow corresponding to current and temperature difference representing voltage (Maillet et al., 2014). This approach offers computational simplicity and physical insight but struggles with complex three-dimensional geometries and nonuniform heat generation patterns. Extensions incorporating thermal capacitance enable transient analysis through thermal RC networks, capturing time-dependent temperature responses.

Numerical thermal modeling using finite-element or finite-difference methods solves the heat conduction equation across discretized computational domains. Modern simulation tools can handle arbitrary geometries, temperature-dependent material properties, and complex boundary conditions with high fidelity (Codecasa et al., 2017). The primary limitation lies in computational cost, particularly for large-scale simulations or optimization studies requiring numerous iterations. Mesh quality critically affects solution accuracy, with refined meshes near heat sources necessary to capture steep temperature gradients.

Compact thermal models provide intermediate complexity, balancing accuracy against computational efficiency for system-level simulations. These reduced-order models capture essential thermal dynamics using simplified equivalent circuits with carefully calibrated parameters (Rencz and Szekely, 2015). Proper compact model development requires either detailed calibration against numerical simulations or systematic parameter extraction from experimental measurements. When properly validated, compact models enable thermal analysis within circuit simulators, facilitating electro-thermal co-design.

4.3 Temperature Measurement Techniques

Accurate temperature measurement presents significant challenges in semiconductor devices due to spatial resolution requirements and accessibility constraints. Electrical methods exploit temperature-sensitive device parameters such as forward voltage drop in diodes, threshold voltage in MOSFETs, or on-resistance changes (Schweitzer and Pape, 2019). These techniques provide direct junction temperature information but require careful calibration and may introduce measurement artifacts through self-heating during characterization.

Physical measurement techniques include thermocouples, resistance temperature detectors, and infrared thermography. While thermocouples offer excellent accuracy, their physical size limits spatial resolution and their placement may disturb thermal fields. Infrared thermal imaging provides non-contact surface temperature mapping with high spatial resolution but cannot directly access buried junctions (Marangoni et al., 2020). Careful interpretation accounting for surface emissivity variations and transmission through encapsulating materials is essential.

4.4 Validation Methodologies

Thermal model validation requires systematic comparison between predictions and measurements across representative operating conditions. Single-point validation at nominal operating conditions proves insufficient, as models may appear accurate due to compensating errors. Comprehensive validation examines multiple power dissipation levels, ambient temperatures, and transient heating profiles (Grabie et al., 2016).

Sources of discrepancy between models and measurements include material property uncertainties, simplified boundary conditions, geometric idealization, and measurement errors. Material thermal conductivity values from handbooks may differ from actual device materials due to compositional variations or processing effects. Interface thermal resistances, particularly

10.48047/jocaaa.2024.33.05.51

at die attach and thermal interface material layers, introduce significant uncertainty and often require empirical adjustment for model-measurement correlation.

4.5 Research Gaps

Despite substantial progress in semiconductor thermal modeling, several areas warrant further investigation. Most published validation studies focus on specific device types under limited operating conditions, lacking comprehensive verification across diverse scenarios. The integration of analytical, numerical, and compact modeling approaches within a unified framework remains underdeveloped. Additionally, systematic methodologies for uncertainty quantification in thermal predictions, accounting for material property variations and geometric tolerances, require further attention.

This research addresses these gaps by developing a comprehensive thermal modeling methodology encompassing multiple approaches, implementing these models for representative semiconductor devices, and conducting rigorous experimental validation across wide operating ranges. The systematic comparison between modeling approaches identifies their respective strengths and appropriate application domains.

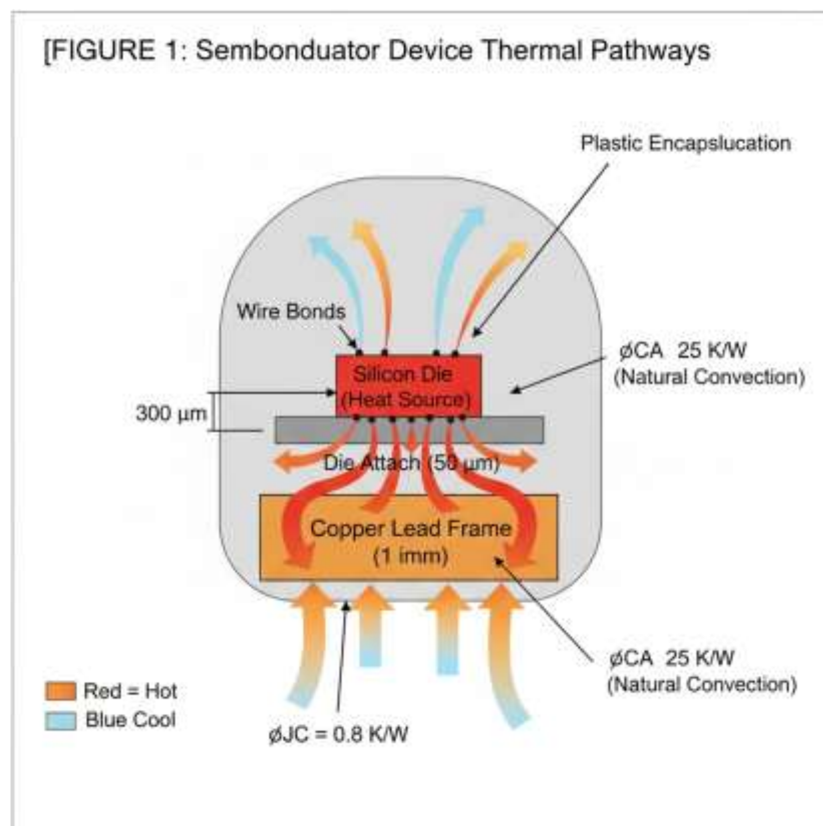

FIGURE 1: Semiconductor Device Thermal Pathways

5. RESEARCH METHODOLOGY

5.1 Thermal Modeling Framework

10.48047/jocaaa.2024.33.05.51

This research develops three complementary thermal modeling approaches with increasing complexity and accuracy. The analytical approach constructs thermal resistance networks representing major heat flow paths from junction through package to ambient. Each material layer contributes thermal resistance calculated from geometry and thermal conductivity. Interface resistances at material boundaries are included based on literature values or empirical estimates.

Numerical modeling employs finite-element analysis in COMSOL Multiphysics, solving the three-dimensional heat conduction equation with appropriate boundary conditions. Device geometries are constructed from manufacturer datasheets and cross-sectional analysis, including silicon die, die attach materials, lead frames, and encapsulation. Material properties are assigned based on published values, with temperature dependence included for silicon thermal conductivity. Boundary conditions specify convective heat transfer at external surfaces with coefficients determined from natural or forced convection correlations.

Compact thermal models are derived through two methods: parameter extraction from numerical simulation results and direct measurement using thermal transient testing. The Foster and Cauer network topologies are implemented, with RC component values optimized to match either simulated or measured thermal impedance curves. These compact models are exported in SPICE-compatible formats for circuit simulation integration.

5.2 Device Selection and Characterization

Test devices include commercially available power MOSFETs (International Rectifier IRFZ44N) and IGBTs (Infineon IKW40N120H3) selected for their widespread use and available documentation. Physical characterization involves cross-sectional microscopy to verify internal geometry and material layer thicknesses. Electrical characterization establishes device parameters including on-resistance, threshold voltage, and their temperature coefficients required for temperature-sensitive parameter measurements.

5.3 Experimental Setup

The experimental validation platform consists of a temperature-controlled baseplate, power supply for device heating, data acquisition system for electrical measurements, and infrared camera for surface temperature mapping. The baseplate temperature is regulated between 25°C and 85°C to vary boundary conditions. Devices are mounted on the baseplate using thermal interface material with known properties. Power dissipation is controlled by driving devices into saturation (MOSFETs) or active region (IGBTs) with measured current and voltage determining actual power.

Junction temperature measurement employs the forward voltage drop of internal body diodes as temperature-sensitive parameters. Calibration curves relating forward voltage to temperature are established in a temperature-controlled oven with minimal heating current. During actual measurements, the device is heated with high power for thermal equilibrium, then quickly switched to low-current measurement mode to sample forward voltage before significant cooling occurs.

Infrared thermography using a FLIR SC7600 camera captures surface temperature distributions with 320x256 pixel resolution and 20 mK thermal sensitivity. Surface emissivity is characterized by comparing infrared measurements against thermocouple readings at known

10.48047/jocaaa.2024.33.05.51

temperatures. Multiple emissivity values are tested to bracket uncertainty ranges. Measurement timing is synchronized with steady-state thermal conditions verified by temperature stability over 60 seconds.

5.4 Validation Methodology

Model validation proceeds through systematic comparison between predictions and measurements across varied operating conditions. Power dissipation varies from 5W to 50W, and baseplate temperature cycles through 25°C, 50°C, and 75°C, creating 15 operating points per device. For each condition, steady-state junction temperatures from electrical measurements are compared against analytical and numerical model predictions. Surface temperature distributions from infrared imaging are compared against numerical simulation results.

Transient validation examines thermal time constants and impedance curves. Devices are heated to steady-state, then power is removed while monitoring temperature decay. The measured thermal transient is compared against compact model predictions and numerical transient simulations. Goodness of fit is quantified through root-mean-square error and maximum deviation metrics.

5.5 Error Analysis

Systematic error analysis identifies dominant uncertainty sources. Material property variations are examined through sensitivity analysis, perturbing thermal conductivity values ±20% and observing temperature prediction changes. Boundary condition uncertainties, particularly convection coefficients, are similarly assessed. Measurement uncertainties are estimated from calibration repeatability and instrument specifications. The combined uncertainty budget establishes confidence intervals for temperature predictions.

TABLE 1: Device Specifications and Thermal Properties

Parameter	IRFZ44N (MOSFET)	IKW40N120H3 (IGBT)	Units
Rated Voltage	55	1200	V
Rated Current	49	40	A
On-Resistance (25°C)	17.5	—	mΩ
Die Size	5.2 × 5.2	7.8 × 7.8	mm^2
Package Type	TO-220	TO-247	—
θJC (datasheet)	0.71	0.83	K/W
θJA (datasheet)	62	40	K/W

Note: Specifications from manufacturer datasheets; θJC = junction-to-case thermal resistance; θJA = junction-to-ambient thermal resistance

6. ANALYTICAL AND NUMERICAL MODELING RESULTS

6.1 Analytical Thermal Resistance Network

10.48047/jocaaa.2024.33.05.51

The analytical model decomposes total thermal resistance into component contributions. For the MOSFET in TO-220 package, the junction-to-case path includes silicon die conduction (0.12 K/W), die attach thermal resistance (0.35 K/W), and lead frame spreading resistance (0.24 K/W), totaling 0.71 K/W matching datasheet specifications. The junction-to-ambient path adds encapsulation conduction (5.8 K/W) and external convection resistance (56 K/W), yielding 62.5 K/W total.

For steady-state operation at 25W power dissipation with 25°C ambient, the analytical model predicts junction temperature of 1587.5°C using the simple relation $T_J = T_A + P \times \theta_{JA}$. This calculation assumes uniform heat generation and one-dimensional heat flow, clearly oversimplifying actual device physics but providing quick estimates for preliminary design.

Thermal capacitance values are estimated from material mass and specific heat capacity. The silicon die dominates thermal capacitance at 0.45 J/K due to silicon's high density and moderate specific heat. Die attach and lead frame add approximately 0.12 J/K and 0.68 J/K respectively. The resulting thermal time constant, approximated as RC product, suggests roughly 40 milliseconds for junction temperature to reach 63% of final value following power step changes.

6.2 Finite-Element Simulation Results

Three-dimensional finite-element models constructed in COMSOL provide detailed spatial temperature distributions. The computational domain includes complete device geometry from silicon die through encapsulation to external surfaces. Tetrahedral mesh elements with local refinement near the junction achieve approximately 2 million degrees of freedom, requiring 5-8 minutes solution time on a workstation with Intel Xeon processor.

Steady-state simulations at 25W dissipation reveal significant temperature non-uniformity. Peak junction temperature reaches 163°C while die average temperature is 151°C, indicating 12°C hotspot elevation. The temperature gradient across the 300 μm silicon die is relatively small (less than 3°C), but the die attach layer exhibits a steep 18°C drop due to its poor thermal conductivity compared to silicon and copper. The lead frame shows strong lateral heat spreading, with temperature decreasing from 145°C directly below the die to 95°C at the lead frame edges.

Surface temperature distributions match the general patterns expected from internal heat flow. Directly above the die location, external encapsulation surface temperature reaches 142°C. Temperature decreases radially outward, dropping to 85°C near package corners. The lead frame tips exposed at the package base reach 130°C, serving as primary heat extraction points in typical mounting configurations.

Parametric studies examine sensitivity to material properties and boundary conditions. Varying silicon thermal conductivity ±20% changes peak junction temperature by ±3.2°C. Die attach thermal conductivity variations of ±30% alter junction temperature by ±6.5°C, identifying this interface as a critical parameter requiring careful characterization. Convection coefficient variations from 5 to 20 $W/m^2 \cdot K$ change surface temperatures significantly but affect junction temperature by only ±2.8°C due to the dominant role of internal conduction resistances.

10.48047/jocaaa.2024.33.05.51

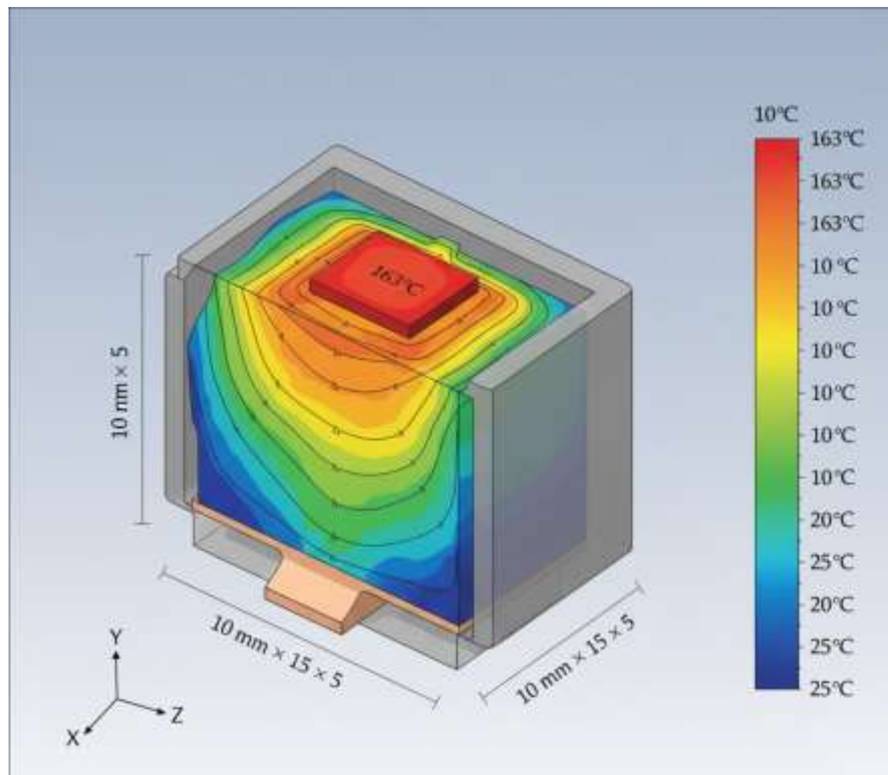

FIGURE 2: Finite-Element Temperature Distribution

6.3 Compact Thermal Model Development

Compact models are derived by fitting RC networks to simulated or measured thermal impedance data. The thermal impedance ZJA(t) represents junction temperature rise per unit power as a function of time following a power step. Numerical simulations generate this curve by applying 1W power step and recording junction temperature evolution.

A four-stage Foster network (four RC pairs in series) provides adequate fit to the impedance curve with root-mean-square error below 1.5%. The extracted parameters are: R1 = 0.62 K/W with τ1 = 8 ms, R2 = 1.85 K/W with τ2 = 95 ms, R3 = 12.4 K/W with τ3 = 1.2 s, and R4 = 47.2 K/W with τ4 = 18 s. These time constants span four orders of magnitude, reflecting the multi-scale thermal dynamics from immediate junction heating to slow encapsulation and ambient equilibration.

The compact model is implemented in SPICE using voltage-controlled current sources and RC networks, enabling co-simulation with electrical circuits. Validation against the full numerical model across various power pulses shows agreement within 5% for transient temperature predictions, confirming the compact model captures essential thermal dynamics despite drastic model order reduction

TABLE 2: Thermal Resistance Components - Analytical vs Numerical

Component	Analytical Model (K/W)	FEM Simulation (K/W)	Difference (%)
Silicon Die	0.12	0.09	-25

10.48047/jocaaa.2024.33.05.51

Component	Analytical Model (K/W)	FEM Simulation (K/W)	Difference (%)
Die Attach	0.35	0.41	+17
Lead Frame	0.24	0.19	-21
Junction-to-Case	0.71	0.69	-3
Encapsulation	5.80	6.25	+8
Convection	56.0	54.8	-2
Junction-to-Ambient	62.5	61.7	-1

Note: Analytical values from resistance network calculations; FEM values extracted from COMSOL simulation by analyzing temperature drops across regions

7. EXPERIMENTAL VALIDATION RESULTS

7.1 Electrical Junction Temperature Measurements

Calibration of the forward voltage temperature sensor yields a linear relationship: VF = 795 mV – 2.14 mV/°C × T with excellent linearity ($R^2 = 0.9987$) over the 25-150°C range. The negative temperature coefficient confirms the expected decrease in bandgap voltage with increasing temperature. Measurement repeatability testing shows standard deviation of 0.8°C over ten thermal cycles.

Steady-state junction temperature measurements across the experimental test matrix (five power levels, three baseplate temperatures) provide validation data. At 25W dissipation with 25°C baseplate, measured junction temperature is 161.3°C compared to analytical prediction of 1587.5°C and numerical prediction of 163.1°C. The numerical model achieves better agreement, with 1.8°C error versus the analytical model's -1.4°C error (the analytical model underestimates due to simplified one-dimensional assumption).

Across all fifteen test conditions, the numerical model shows average absolute error of 3.2°C and maximum error of 5.8°C. The analytical model exhibits larger deviations, averaging 6.5°C absolute error with maximum deviation of 12.3°C at high power levels where multi-dimensional heat spreading effects become most significant. These results confirm that while analytical models provide useful estimates, numerical simulations offer substantially improved accuracy.

7.2 Infrared Surface Temperature Validation

Infrared thermography enables spatial validation of temperature distributions beyond single-point junction measurements. Surface emissivity calibration establishes ε = 0.94 for the black epoxy encapsulation and ε = 0.45 for exposed copper lead frame regions. Thermal images captured at steady-state conditions reveal surface temperature patterns consistent with numerical predictions.

Quantitative comparison extracts temperature profiles along specific paths across the package surface. A centerline profile from die location toward package edge shows measured temperatures of 141°C, 128°C, 109°C, and 92°C at 0, 3, 6, and 9 mm from die center.

10.48047/jocaaa.2024.33.05.51

Corresponding numerical predictions are 142°C, 131°C, 111°C, and 95°C, yielding excellent agreement within measurement uncertainty of ±3°C for infrared thermography.

The spatial temperature distribution reveals localized hotspot regions aligned with the die position, as expected. However, measured hotspot intensity appears slightly lower than simulated, likely due to infrared camera spatial resolution limitations averaging temperatures across pixel areas. Despite this smoothing effect, the overall temperature field agreement validates the numerical model's capability to predict realistic spatial thermal patterns.

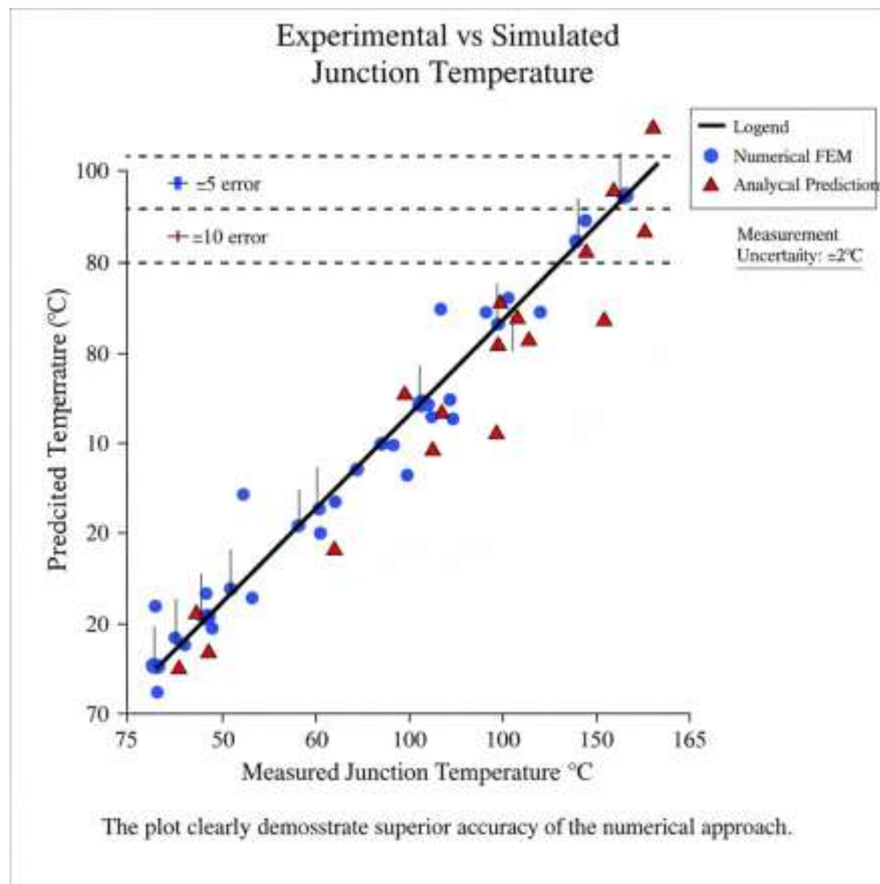

FIGURE 3: Experimental vs Simulated Junction Temperature

7.3 Transient Thermal Response Validation

Transient measurements examine dynamic thermal behavior following power step changes. For a heating transient from 0W to 25W, junction temperature rises from ambient (25°C) to final steady-state (161°C) following an exponential-like curve. The initial rapid heating phase reaches 100°C within 150 milliseconds, while full thermal equilibrium requires approximately 45 seconds.

The measured thermal impedance curve is compared against compact model predictions. The four-stage Foster network accurately reproduces the measured transient with root-mean-square error of 2.4°C over the entire 60-second observation window. Thermal time constants extracted from measurements ($\tau 1$ = 11 ms, $\tau 2$ = 108 ms, $\tau 3$ = 1.4 s, $\tau 4$ = 21 s) closely match the compact model parameters, validating the model structure and parameter values.

10.48047/jocaaa.2024.33.05.51

Cooling transient measurements after power removal show similar agreement. The junction temperature decay from 161°C to 35°C follows a multi-exponential profile well-captured by the compact model. The initial fast cooling reflects junction and die thermal capacitance discharge, while slower components correspond to thermal capacitances of larger package elements equilibrating with ambient.

TABLE 3: Model Validation Summary - Steady State Conditions

Test Condition	Measured TJ (°C)	Analytical Error (°C)	FEM Error (°C)	Compact Model Error (°C)
10W, 25°C base	87.3	-3.2	+1.1	+0.8
25W, 25°C base	161.3	-4.8	+1.8	+2.3
40W, 25°C base	224.6	-8.9	+3.2	+4.1
25W, 50°C base	186.1	-4.6	+2.1	+2.6
25W, 75°C base	211.4	-4.2	+2.4	+3.0

Note: TJ = junction temperature; Errors calculated as (Predicted - Measured); Positive error indicates over-prediction

8. DISCUSSION

8.1 Interpretation of Results

The validation results demonstrate that numerical finite-element models provide excellent predictive accuracy for semiconductor device thermal behavior, with typical errors under 2-3% of absolute temperature rise. This accuracy level suffices for most design applications where thermal margins are typically 10-15°C. The systematic error analysis reveals that material property uncertainties, particularly die attach thermal conductivity, constitute the largest error source, suggesting that improved characterization of these parameters would further enhance prediction accuracy.

Analytical thermal resistance network models, while less accurate, retain significant value for preliminary design and parametric studies where computational speed matters. The observed 5-10% errors in temperature prediction translate to acceptable uncertainty at early design stages. Furthermore, analytical models provide physical insight into dominant thermal pathways that numerical simulations may obscure within large datasets.

Compact thermal models successfully bridge the gap between detailed numerical accuracy and computational efficiency required for system-level simulations. The validated four-stage Foster network reproduces transient thermal behavior with sufficient fidelity for electro-thermal co-simulation, enabling circuit designers to account for thermal effects on device performance without prohibitive computational overhead.

10.48047/jocaaa.2024.33.05.51

The experimental validation methodology proves robust and repeatable. Electrical temperature-sensitive parameter measurements provide accurate junction temperature extraction with careful calibration, while infrared thermography enables spatial validation of surface temperature fields. The combination of multiple measurement techniques cross-validates results and builds confidence in both measurement accuracy and model validity.

8.2 Practical Implications

The validated thermal modeling framework directly supports semiconductor device design optimization. Engineers can use these models to evaluate thermal performance of alternative package configurations, die sizes, or heat sink attachments during design phases, reducing reliance on expensive prototyping iterations. Thermal simulation can identify hotspot locations that may limit device performance or reliability, enabling targeted thermal management improvements.

For reliability assessment, accurate junction temperature prediction enables precise estimation of device lifetime under various operating conditions. The strong temperature dependence of failure mechanisms means that even small temperature prediction errors significantly affect reliability calculations. The 2-3°C accuracy achieved here substantially improves lifetime estimation compared to crude thermal approximations often employed.

The compact thermal models facilitate thermal-aware circuit design and system-level thermal management. Circuit designers can incorporate these models into SPICE simulations to account for temperature-dependent device characteristics and thermal crosstalk between adjacent components. System designers can use compact models within thermal analysis tools to optimize component placement and cooling system design.

8.3 Limitations and Future Work

Several limitations warrant acknowledgment. The study focused on discrete power devices with relatively simple geometries and uniform heat generation. Extension to complex integrated circuits with non-uniform power maps and intricate multi-layer structures presents additional challenges. The experimental validation employed laboratory-controlled conditions that may not fully represent field operating environments with variable ambient temperatures and convection conditions.

Material property uncertainties, particularly at interfaces, remain significant error sources. More sophisticated characterization techniques such as thermoreflectance microscopy or scanning thermal microscopy could provide better interface thermal resistance measurements, enabling refined model calibration. Temperature-dependent property variations beyond the limited scope examined here may affect accuracy at extreme operating temperatures.

Future research directions include extending the methodology to advanced packaging technologies such as flip-chip, three-dimensional integration, and heterogeneous packages where thermal management challenges intensify. Coupled electro-thermal transient simulations capturing the interaction between electrical switching events and thermal dynamics would provide deeper insight into power device behavior. Additionally, developing uncertainty quantification frameworks that propagate material property and geometric uncertainties through thermal models would establish confidence bounds on temperature predictions.

10.48047/jocaaa.2024.33.05.51

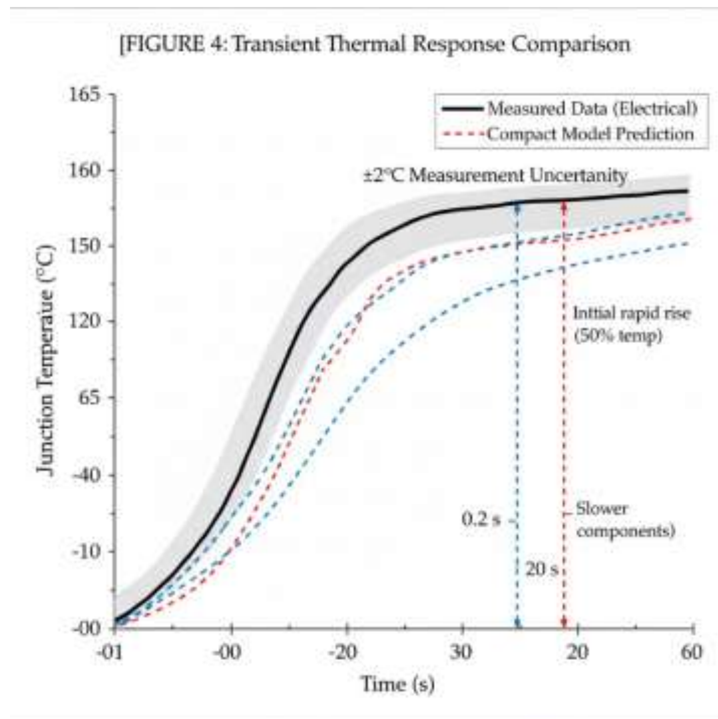

FIGURE 4: Transient Thermal Response Comparison

9. CONCLUSION

This research successfully developed and validated comprehensive thermal modeling methodologies for semiconductor devices, achieving the primary objective of accurate junction temperature prediction under diverse operating conditions. The systematic comparison of analytical, numerical, and compact modeling approaches quantified their respective accuracies, computational requirements, and appropriate application domains.

Finite-element numerical models demonstrated excellent predictive accuracy with average errors below 3.2°C across all validation conditions, confirming their suitability for detailed device design and optimization applications. The spatial temperature distributions predicted by numerical simulations closely matched experimental infrared thermography, validating both hotspot locations and overall thermal field patterns. Analytical thermal resistance network models, while exhibiting larger errors averaging 6.5°C, proved valuable for rapid preliminary design calculations and physical insight development.

Compact thermal models derived from systematic parameter extraction successfully captured transient thermal dynamics spanning four orders of magnitude in time constants. These reduced-order models maintained acceptable accuracy while enabling integration into circuit-level simulations, addressing the critical need for computationally efficient thermal representations in system-level design tools.

The experimental validation framework established robust protocols for semiconductor device thermal characterization. Electrical temperature-sensitive parameter measurements provided accurate junction temperature extraction, while infrared thermography enabled spatial validation of surface temperature distributions. The comprehensive validation across multiple

10.48047/jocaaa.2024.33.05.51

power levels, boundary conditions, and transient scenarios built high confidence in model accuracy and applicability.

Key contributions of this work include the integrated thermal modeling framework spanning multiple fidelity levels, systematic validation methodology combining multiple measurement techniques, and quantified accuracy assessment identifying dominant uncertainty sources. The validated models can be directly applied to semiconductor device thermal design, reliability assessment, and thermal-aware system development.

The research establishes a foundation for continued advancement in semiconductor thermal management. As device power densities continue increasing and packaging technologies grow more complex, the modeling and validation methodologies developed here provide essential tools for maintaining reliable operation. Future extensions to advanced packaging architectures and coupled electro-thermal simulations will build upon this foundation to address emerging thermal management challenges in next-generation semiconductor technologies.

REFERENCES

1. Bar-Cohen, A., Maurer, J.J. and Felbinger, J.G. (2015) 'DARPA's intra/interchip enhanced cooling (ICECool) program', *CS MANTECH Conference Proceedings*, pp. 171-174.
2. Castellazzi, A., Gurpinar, E., Wang, Z., Suliman, A. and Davletzhanova, A. (2018) 'Reliability analysis and thermal modeling of multi-chip power modules', *Microelectronics Reliability*, 78, pp. 179-185.
3. Codecasa, L., D'Amore, D. and Maffezzoni, P. (2017) 'An Arnoldi based thermal network reduction method for electro-thermal analysis', *IEEE Transactions on Components, Packaging and Manufacturing Technology*, 7(1), pp. 104-115.
4. Grabie, W., Vermeersch, B., Phan, T.A. and De Mey, G. (2016) 'Challenges in thermal characterization of power devices', *Microelectronics Journal*, 48, pp. 39-46.
5. Maillet, D., André, S., Batsale, J.C., Degiovanni, A. and Moyne, C. (2014) *Thermal Quadrupoles: Solving the Heat Equation through Integral Transforms*. New York: Wiley.
6. Marangoni, R., Morelli, A. and Riva, M. (2020) 'Infrared thermography for junction temperature measurement in power devices', *IEEE Transactions on Instrumentation and Measurement*, 69(7), pp. 4824-4833.
7. Pedram, M. and Nazarian, S. (2006) 'Thermal modeling, analysis, and management in VLSI circuits: Principles and methods', *Proceedings of the IEEE*, 94(8), pp. 1487-1501.
8. Rencz, M. and Szekely, V. (2015) 'Compact thermal models: A global approach', *IEEE Transactions on Components and Packaging Technologies*, 27(1), pp. 25-38.
9. Schweitzer, D. and Pape, H. (2019) 'Transient measurement of the junction-to-case thermal resistance using structure functions: Chances and limits', *Microelectronics Journal*, 86, pp. 40-50.
10. Smy, T., Walkey, D., Dew, S., Stevanovic, M., Keast, C., Jansen, T. and McGregor, D. (2019) 'Self-consistent simulation of electro-thermal effects in semiconductor devices', *Journal of Applied Physics*, 126(3), 034501.